Synthesis and Characterization of an Asymmetric Bridged Assembly Containing the Unsupported [Fe^{III}–O–Cu^{II}] Bridge: An Analogue of the Binuclear Site in Oxidized Cytochrome *c* Oxidase

Sonny C. Lee[1] and R. H. Holm*

Contribution from the Department of Chemistry, Harvard University, Cambridge, Massachusetts 02138

*Received August 2, 1993**

Abstract: A synthetic analogue of the antiferromagnetically coupled $S = 2$ Fe/Cu binuclear site in oxidized (as-isolated) cytochrome *c* oxidase has been sought. Initial Cu(II) precursor compound $[Cu(Me_6tren)(OH_2)](ClO_4)_2$ containing the trigonal bipyramidal (TBP) complex $[1]^{2+}$ upon treatment with methanolic KOH yields $[Cu(Me_6tren)(OH)]^+$ ($[2]^+$) with TBP stereochemistry and a terminal hydroxo group. In acetone solution, reaction of $[1]^{2+}$ with 2 equiv of the hindered base lithium 2,6-di-*tert*-butyl-4-methylphenolate and 1 equiv of $[Fe(OEP)(OClO_3)]$ affords (via the presumed intermediate $[2]^+$) the bridged assembly $[(OEP)Fe–O–Cu(Me_6tren)]^+$ ($[3]^+$) in 67% isolated yield as the perchlorate salt (**3**). A coproduct is the previously unknown high-spin enolate complex $[Fe(OEP)(OC(Me)=CH_2)]$, identified by ^1H NMR. The effects of solvent and base on the formation of $[3]^+$ are considered. Compounds **3**·MeCN and **3**·THF crystallize in monoclinic and orthorhombic space groups, respectively, with the former having two inequivalent molecules in the asymmetric unit; the structures of $[3]^+$ in three different crystalline environments are essentially invariant. Tetragonal five-coordinate Fe(III) is linked to TBP Cu(II) by the asymmetric, unsupported, nearly linear Fe–O–Cu bridge (mean angle 176.6°). The presence of high-spin Fe(III) is supported by structural and Mössbauer spectroscopic parameters. Magnetic susceptibility data at 4-300 K for polycrystalline **3** can be fitted well to Curie–Weiss behavior corresponding to $S = 2$, which must arise from antiferromagnetic coupling between $S = 5/2$ and $1/2$ centers. Retention of this bridge in acetone solution is indicated by diastereotopic methylene proton resonances whose isotropic shifts are smaller than those of high-spin Fe(III) hemes. Bridged assembly $[3]^+$ reproduces the most prominent electronic feature of the oxidized enzyme site and in this sense is the first synthetic analogue of that site.

Introduction

The oxygen/water redox couple, reaction 1 in Figure 1, serves as the junction that links the divergent biochemical pathways of respiration and photosynthesis. In biology, the forward process—the terminus of the respiratory chain, an exergonic sequence of chemically coupled electron transfers—is catalyzed by the terminal oxidases, eukaryotic cytochrome *c* oxidase (CcO) and related prokaryotic variants, enzymes that tie the reduction of dioxygen to energy conversion by concomitant proton translocation against a trans-membrane concentration gradient.[2] All terminal oxidases are necessarily membrane-associated in light of their proton-pumping function, with the eukaryotic enzymes bound to the inner mitochondrial membrane and their prokaryotic analogues attached to the plasma membrane. With the respiratory chain providing most of the free energy required in aerobic organisms, the terminal oxidases are critical biochemical components and, as such, CcO, the most accessible member of the family, has been the subject of extensive study.

Cytochrome *c* oxidase possesses four well-defined transition metal centers, consisting of two heme and two copper sites. Their relative positions are schematically represented in Figure 1. Heme *a*, which is low-spin with bis(imidazole) axial ligation,[3] and the Cu_A site, believed to possess bis(imidazole) disulfur ligation,[4,5] probably act as electron-transfer centers. There is evidence to suggest that the Cu_A site is actually binuclear.[4c] Although related prokaryotic enzymes display variation at these two sites, with one subclass (quinol oxidases) lacking Cu_A altogether, all enzymes exhibit the same functionality, ruling out heme *a* and Cu_A as centers of substrate transformation. The catalytic core of CcO is defined by the remaining two metal sites, heme a_3 and Cu_B, which are proximally associated to form the bimetallic reaction center directly responsible for dioxygen reduction and critically linked to proton translocation. EPR experiments with ^{15}N-labeled histidine and exogenous probe ligands show hyperfine structure indicative of axial imidazole ligation at heme a_3 on the face distal to Cu_B.[6] ENDOR spectroscopy of an EPR-active form of Cu_B suggests that it possesses a coordination sphere similar to the type 3 copper site in laccase, minimally defined by at least three imidazole ligands from histidine residues.[7] The ligand assignments are supported by protein sequence analysis of the subunit containing the two hemes and Cu_B; at least six histidine residues are conserved in all known terminal oxidases, providing two for heme *a*, one for heme a_3, and three for Cu_B.[2d]

The structure of the binuclear active site has been deduced primarily from studies of the oxidized enzyme "as-isolated" from protein purification. Critical observations concerning the bimetallic center in this as-isolated state include the following.

(1) EPR. The oxidized enzyme presumably possesses two Fe(III) and two Cu(II) sites, all of which should be EPR-active. No

* Abstract published in *Advance ACS Abstracts*, November 15, 1993.

(1) National Science Foundation Predoctoral Fellow, 1987–1990.

(2) (a) Babcock, G. T.; Wikström, M. *Nature* **1992**, *356*, 301. (b) Chan, S. I.; Li, P. M. *Biochemistry* **1990**, *29*, 1. (c) Malmström, B. G. *Chem. Rev.* **1990**, *90*, 1247; *Acc. Chem. Res.* **1993**, *26*, 332. (d) Capaldi, R. A. *Annu. Rev. Biochem.* **1990**, *59*, 569.

(3) Martin, C. T.; Scholes, C. P.; Chan, S. I. *J. Biol. Chem.* **1985**, *260*, 2857.

(4) (a) Stevens, T. H.; Martin, C. T.; Wang, H.; Brudvig, G. W.; Scholes, C. P.; Chan, S. I. *J. Biol. Chem.* **1982**, *257*, 12106. (b) Martin, C. T.; Scholes, C. P.; Chan, S. I. *J. Biol. Chem.* **1988**, *263*, 8420. (c) Malmström, B. G.; Aasa, R. *FEBS Lett.* **1993**, *325*, 49. (d) See also: Kelly, M.; Lappalainen, P.; Talbo, G.; Haltia, T.; van der Oost, J.; Saraste, M. *J. Biol. Chem.* **1993**, *268*, 16781.

(5) George, G. N.; Cramer, S. P.; Frey, T. G.; Prince, R. C. *Biochim. Biophys. Acta* **1993**, *1142*, 240.

(6) Stevens, T. H.; Chan, S. I. *J. Biol. Chem.* **1981**, *256*, 1069.

(7) Cline, J.; Reinhammer, B.; Jensen, P.; Venters, R.; Hoffman, B. M. *J. Biol. Chem.* **1983**, *258*, 5124.

0002-7863/93/1515-11789$04.00/0

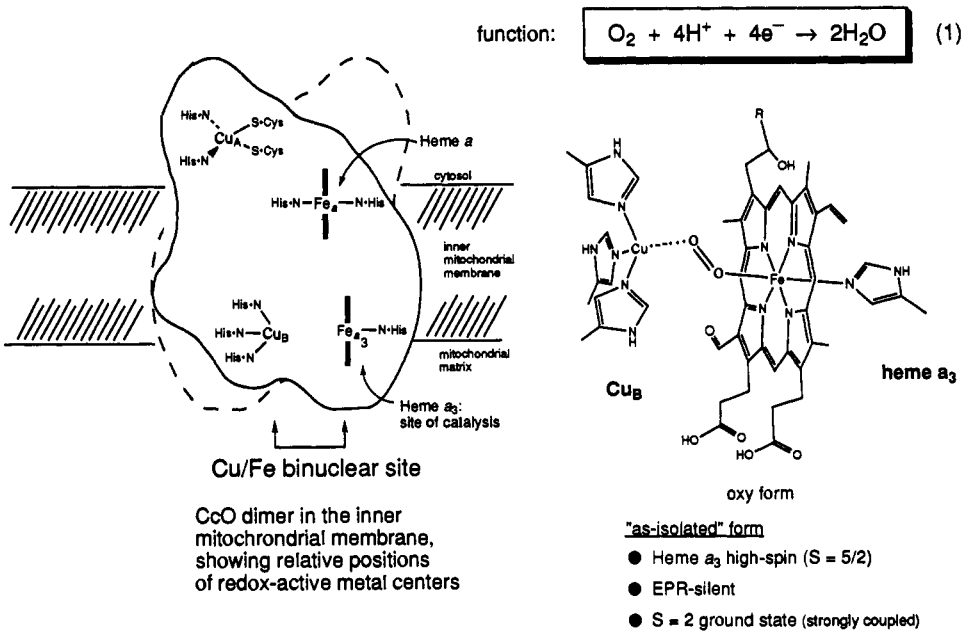

Figure 1. Description of cytochrome *c* oxidase, including schematic representations of the relative positions of redox centers in the CcO dimer (adpated from ref 2b) and of the Cu–Fe binuclear site in the oxy form, and the leading properties of the "as-isolated" form of the enzyme. Note that the Cu_A site may be binuclear.[4c]

odd-spin EPR signal is detectable from either heme a_3 or Cu_B in the as-isolated state.[8]

(2) Magnetic Susceptibility. Data from variable temperature susceptibility measurements, after subtraction of the contributions from heme *a* and Cu_A, indicate that the remaining paramagnetism is best fit by a single entity of spin $S = 2$; moreover, the $S = 2$ contributor exhibits Curie behavior, extrapolating linearly to room temperature.[9]

(3) Mössbauer,[10] Resonance Raman,[11] and MCD[12] Spectroscopies. All data from these methods indicate a high-spin Fe(III) state ($S = 5/2$) for heme a_3; Cu_B, when cupric, necessarily has $S = 1/2$. Resonance Raman data indicate that the Fe(III) atom is six-coordinate.[11a]

These observations are accounted for in the standard model of the oxidized binuclear site by invoking an antiferromagnetic interaction between heme a_3 and Cu_B to yield a $S = 2$ system spin. Propagation of such an interaction requires the two metals to be closely spaced and covalently bridged. In terms of our recent definitions of binuclear bridges,[13] the binuclear site itself must be an asymmetric, intimately bridged assembly. Furthermore, recent magnetic data suggest that the electronic coupling is unperturbed to at least 200 K, indicating a moderate to strong interaction with $-J \geq 50$ cm^{-1} [9d] (as described under the Hamiltonian $H = -2JS_1S_2$). Site probes with exogenous ambidentate ligands (e.g., CN^-,[10,14] NO[15]) have also yielded spectroscopic data indicative of ligand bridging. Certain exogenous ligands have been found to induce EPR signals from the "silent" metal centers, suggesting that these species uncouple, or perturb the coupling of, the bridged assembly.[16]

The identity of the bridging ligand in the as-isolated state remains unresolved. Independent X-ray absorption studies by two groups produce incongruent pictures of the binuclear site in this state.[17] The most recent Cu EXAFS data suggest a Cu–Fe separation of 3.0 Å, but this could not be confirmed from Fe EXAFS owing to intense Fe–C(heme) scattering.[5] Interpretations of spectroscopic results must be considered in light of multiple enzyme conformations and attendant potential inhomogeneities in the binuclear site.[2,16]

In a recent advance, time-resolved resonance Raman spectroscopy has facilitated direct observation of key intermediates in the dioxygen reduction sequence of CcO.[18] While dioxygen activation is generic to a variety of heme enzymes, the binuclear site configuration remains unique to terminal oxidases. The singular characteristics of this reaction center have made it a prime candidate for elucidation by the synthetic analogue approach. Attempts to produce an accurate site mimic, ongoing for 15 years,[19-27] have not met the desired goal of reproducing the observable signatures of any CcO state.[27b] In this connection,

(8) (a) Hartzell, C. R.; Hansen, R. E.; Beinert, H. *Proc. Natl. Acad. Sci. U.S.A.* **1973**, *70*, 2477. (b) Brudvig, G. W.; Morse, R. H.; Chan, S. I. *J. Magn. Reson.* **1986**, *67*, 189.

(9) (a) Tweedle, M. F.; Wilson, L. J.; Garcia-Iñiguez, L.; Babcock, G. T.; Palmer, G. *J. Biol. Chem.* **1978**, *253*, 8065. (b) Moss, T. H.; Shapiro, E.; King, T. E.; Beinert, H.; Hartzell, C. *J. Biol. Chem.* **1978**, *253*, 8072. (c) Barnes, Z. K.; Babcock, G. T.; Dye, J. L. *Biochemistry* **1991**, *30*, 7597. (d) Day, E. P.; Peterson, J.; Sendova, M. S.; Schoonover, J.; Palmer, G. *Biochemistry* **1993**, *32*, 7855.

(10) (a) Kent, T. A.; Young, L. J.; Palmer, G.; Fee, J. A.; Münck, E. *J. Biol. Chem.* **1983**, *258*, 8543. (b) Kent, T. A.; Münck, E.; Dunham, W. R.; Filter, W. F.; Findling, K. L.; Yoshida, T.; Fee, J. A. *J. Biol. Chem.* **1982**, *257*, 12489. See also: (c) Wang, H.; Sauke, T.; Debrunner, P. G.; Chan, S. I. *J. Biol. Chem.* **1988**, *263*, 15260.

(11) (a) Babcock, G. T.; Callahan, P. M.; Ondrias, M. R.; Selmeen, I. *Biochemistry* **1981**, *20*, 959. (b) Woodruff, W. H.; Dallinger, R. F.; Antalis, T. M.; Palmer, G. *Biochemistry* **1981**, *20*, 1332.

(12) (a) Babcock, G. T.; Vickery, L. E.; Palmer, G. *J. Biol. Chem.* **1976**, *251*, 7907. (b) Eglinton, D. G.; Johnson, M. K.; Thomson, A. J.; Gooding, P. E.; Greenwood, C. *Biochem. J.* **1980**, *191*, 319.

(13) Lee, S. C.; Holm, R. H. *Inorg. Chem.* **1993**, *32*, 4745. ($bnpy_2$ = *N,N*-bis(2-(2-pyridyl)ethyl)benzylamine.

(14) Thomson, A. J.; Greenwood, C.; Gadsby, P. M. A.; Peterson, J.; Eglinton, D. G.; Hill, B. C.; Nicholls, P. *J. Inorg. Biochem.* **1985**, *23*, 187.

(15) Stevens, T. H.; Brudvig, G. W.; Bocian, D. F.; Chan, S. I. *Proc. Natl. Acad. Sci. U.S.A.* **1979**, *76*, 3320.

(16) Brudvig, G. W.; Stevens, T. H.; Morse, R. H.; Chan, S. I. *Biochemistry* **1981**, *20*, 3912.

(17) Scott, R. A. *Annu. Rev. Biophys. Biophys. Chem.* **1989**, *18*, 137.

(18) Varotsis, C.; Zhang, Y.; Appelman, E. H.; Babcock, G. T. *Proc. Natl. Acad. Sci. U.S.A.* **1993**, *90*, 237.

(19) (a) Prosperi, T.; Tomlinson, A. A. G. *J. Chem. Soc., Chem. Commun.* **1979**, 196. (b) Dessens, S. E.; Merrill, C. L.; Saxton, R. J.; Ilaria, R. L., Jr.; Lindsey, J. W.; Wilson, L. J. *J. Am. Chem. Soc.* **1982**, *104*, 4357. (c) Saxton, R. J.; Wilson, L. J. *J. Chem. Soc., Chem. Commun.* **1984**, 359. (d) Brewer, C. T.; Brewer, G. A. *Inorg. Chem.* **1987**, *26*, 3420. (e) Koch, C. A.; Reed, C. A.; Brewer, G. A.; Rath, N. P.; Scheidt, W. R.; Gupta, G.; Lang, G. *J. Am. Chem. Soc.* **1989**, *111*, 7645. (f) Gupta, G. P.; Lang, G.; Koch, C. A.; Wang, B.; Scheidt, W. R.; Reed, C. A. *Inorg. Chem.* **1990**, *29*, 4234. (g) Wang, R.; Brewer, G. *Inorg. Chim. Acta* **1993**, *206*, 117.

Table I. Crystallographic Data[a] for [Cu(Me$_6$tren)(OH$_2$)](ClO$_4$)$_2$ (**1**), [Cu(Me$_6$tren)(OH)](ClO$_4$)$_2$·H$_2$O (**2**), [(OEP)Fe–O–Cu(Me$_6$tren)](ClO$_4$)·MeCN (**3**·MeCN), and [(OEP)Fe–O–Cu(Me$_6$tren)](ClO$_4$)·THF (**3**·THF)

	1	**2**	**3**·MeCN	**3**·THF
formula	$C_{12}H_{32}Cl_2CuN_4O_9$	$C_{12}H_{33}ClCuN_4O_6$	$C_{50}H_{77}ClCuFeN_9O_5$	$C_{52}H_{82}ClCuFeN_8O_6$
formula wt	510.93	428.49	1039.21	1070.27
crystal system	monoclinic	orthorhombic	monoclinic	orthorhombic
a, Å	17.367(4)	8.479(2)	17.847(3)	15.044(2)
b, Å	13.011(3)	14.498(2)	25.085(4)	18.296(3)
c, Å	18.992(4)	16.120(3)	25.356(4)	20.051(3)
α, deg	90	90	90	90
β, deg	93.45(2)	90	108.95(1)	90
γ, deg	90	90	90	90
V, Å^3	4284(2)	1982(1)	10736(3)	5519(1)
space grou	$P2_1/c$ (no. 14)	$P2_12_12_1$ (no. 19)	$P2_1/n$ (no. 14)	$Pnma$ (no. 62)
z	8	4	8	4
ρ_{calc}, g/cm^3	1.58	1.44	1.29	1.29
μ, mm^{-1}	1.32	1.27	0.77	0.75
R^b (R_w^c), %	8.02 (6.62)	3.32 (4.02)	8.47 (8.00)	5.53 (6.10)

[a] All data collected at T = 173 K with graphite monochromatized Mo Kα radiation (λ = 0.71069 Å) using ω scans. [b] $R = \sum||F_o| - |F_c||/\sum|F_o|$. [c] $R_w = (\sum[w(|F_o| - |F_c|)^2]/\sum(w|F_o|^2))^{1/2}$, with the weighting scheme provided by a three-term Chebyshev polynomial: Carruthers, J. R.; Watkin, D. J. *Acta Crystallogr.* **1979**, *A35*, 698.

the large majority of synthetic binuclear species lack structural proof, preventing a conclusive identification of the bridging unit, with ensuing correlation to electronic behavior. In such a situation, these species remain almost as tentatively defined as the enzyme site itself. We have taken up the CcO site problem by the synthesis and characterization of Fe–Cu unsupported bridged assemblies.[13,28] This article provides a full account of our work on an oxo-bridged assembly, which has been briefly described elsewhere.[28]

Experimental Section

Preparation of Compounds. Compounds **1** and **2** were prepared in air. The synthesis of compound **3** was carried out under a pure dinitrogen atmosphere; ether and THF, distilled from sodium benzophenone ketyl, and acetone, distilled from B_2O_3, were degassed and stored under dinitrogen. Lithium 2,6-di-*tert*-butyl-4-methylphenolate was prepared by the deprotonation of the phenol in hexane with BuLi and was isolated by filtration followed by washings with hexane and drying in vacuo.

[Cu(Me$_6$tren)(OH$_2$)](ClO$_4$)$_2$ (1). A published procedure[29] was followed with modifications. A solution of 2.31 g (10.0 mmol) of Me$_6$tren[29] in 20 mL of ethanol was added to a hot solution of 3.71 g (10.0 mmol) of Cu(ClO$_4$)$_2$·6H$_2$O in 40 mL of ethanol. The initial pale blue color intensified to give a dark blue color at the end of the addition. The solution was brought to a boil and filtered while hot to remove insoluble copper-containing material. After it was cooled to room temperature, the solution was stored at –20 °C for at least 24 h to yield a fused blue crystalline mass. This material was broken up and filtered. The solid was washed with ethanol, followed by ether, to yield 4.36 g (85%) of product as a blue crystalline solid.

[Cu(Me$_6$tren)(OH)](ClO$_4$)·H$_2$O (2). A methanolic KOH solution (13 mg of 85% hydrated KOH in 5 mL of methanol) was added to a solution of 100 mg (0.20 mmol) of **1** in 10 mL of methanol, intensifying the blue solution color. After the solution was stirred for 15 min, it was reduced to a blue syrup by rotary evaporation; dissolution in acetonitrile resulted in a green solution. (The blue color can be restored by adding a protic solvent (methanol, water) to the solution). Diffusion of ether into the concentrated acetonitrile solution yielded an abundant blue-green sticky residue and some blue crystals, which were identified by an X-ray structural determination.

[(OEP)Fe–O–Cu(Me$_6$tren)](ClO$_4$) (3). A blue solution of 371 mg (0.73 mmol) of aquo complex **1** in 25 mL of acetone was added to 330 mg (1.46 mmol) of lithium 2,6-di-*tert*-butyl-4-methylphenolate to give a dark green solution. Addition to 500 mg (0.73 mmol) of solid [Fe(OEP)(OClO$_3$)][30] produced a dark purple-red solution, which was stirred for 30 min. Addition of ether (*ca.* 150 mL) afforded a red microcrystalline precipitate, which was isolated, redissolved in THF (200 mL), and filtered to remove insoluble green copper-containing residues. The solvent was removed in vacuo to give a microcrystalline residue; dissolution in a minimal volume of acetonitrile (*ca.* 20 mL) followed by addition of ether (*ca.* 20 mL) yielded 485 mg (67%) of product as violet microcrystals. Atom ratios Fe:Cu:Cl = 1:1.0:1.1 by microprobe analysis. Absorption spectrum (CH_2Cl_2): λ_{max} (ϵ_M) 286 (18 300), 342 (sh, 35 200), 371 (43 700), 427 (74 700), 499 (sh, 4000), 541 (11 600), 574 (12 700), 634 (1500). ^{1}H NMR (d_6-acetone, 298 K): δ 20.0 and 17.4 (CH_2), 3.63 (CH_3), –16.3 (br CH), –42 (v br). All but the last feature arise from OEP.

Solution and Refinement of Structures. Atom scattering factors were taken from a standard source.[31] The initial structural solutions were obtained by automated interpretation of Patterson maps (XS from the SHELXTL package). Atoms not located from the initial structure solution were found by successive Fourier or difference Fourier maps with intervening cycles of least-squares refinement (CRYSTALS, with graphical interface provided by XP from SHELXTL). Parallel refinement

(20) (a) Petty, R. H.; Wilson, L. J. *J. Chem. Soc., Chem. Commun.* **1978**, 483. (b) Petty, R. H.; Welch, B. R.; Wilson, L. J.; Bottomley, L. A.; Kadish, K. M. *J. Am. Chem. Soc.* **1980**, *102*, 611.

(21) (a) Berry, K. J.; Gunter, M. J.; Murray, K. S. In *Oxygen and Life*; Spec. Publ. No. 39; The Royal Society of Chemistry: London, 1980; pp 170–179. (b) Gunter, M. J.; Mander, L. N.; McLaughlin, G. M.; Murray, K. S.; Berry, K. J.; Clark, P. E.; Buckingham, D. A. *J. Am. Chem. Soc.* **1980**, *102*, 1470. (c) Berry, K. J.; Clark, P. E.; Gunter, M. J.; Murray, K. S. *Nouv. J. Chim.* **1980**, *4*, 581. (d) Gunter, M. J.; Mander, L. N.; Murray, K. S.; Clark, P. E. *J. Am. Chem. Soc.* **1981**, *103*, 6784.

(22) (a) Gunter, M. J.; Mander, L. N.; Murray, K. S. *J. Chem. Soc., Chem. Commun.* **1981**, 799. (b) Saxton, R. J.; Olson, L. W.; Wilson, L. J. *J. Chem. Soc., Chem. Commun.* **1982**, 984. (c) Chang, C. K.; Koo, M. S.; Ward, B. *J. Chem. Soc., Chem. Commun.* **1982**, 716.

(23) Elliott, C. M.; Jain, N. C.; Cranmer, B. K.; Hamburg, A. W. *Inorg. Chem.* **1987**, *26*, 3655.

(24) Gunter, M. J.; Berry, K. J.; Murray, K. S. *J. Am. Chem. Soc.* **1984**, *106*, 4227.

(25) (a) Elliott, C. M.; Akabori, K. *J. Am. Chem. Soc.* **1982**, *104*, 2671. (b) Schauer, C. K.; Akabori, K.; Elliott, C. M.; Anderson, O. P. *J. Am. Chem. Soc.* **1984**, 106, 1127. (c) Serr, B. R.; Headford, C. E. L.; Elliott, C. M.; Anderson, O. P. *J. Chem. Soc., Chem. Commun.* **1988**, 92. (d) Serr, B. R.; Headford, C. E. L.; Anderson, O. P.; Elliott, C. M.; Schauer, C. K.; Akabori, K.; Spartalian, K.; Hatfield, W. E.; Rohrs, B. R. *Inorg. Chem.* **1990**, *29*, 2663. (e) Serr, B. R.; Headford, C. E. L.; Anderson, O. P.; Elliott, C. M.; Spartalian, K.; Fainzilberg, V. E.; Hatfield, W. E.; Rohrs, B. B.; Eaton, S. S.; Eaton, G. R. *Inorg. Chem.* **1992**, *31*, 5450.

(26) (a) Deardorff, E. A.; Carr, P. A. G.; Hurst, J. K. *J. Am. Chem. Soc.* **1981**, *103*, 6616. (b) Lukas, B.; Miller, J. R.; Silver, J.; Wilson, M. T.; Morrison, I. E. G. *J. Chem. Soc., Dalton Trans.* **1982**, 1035. (c) Cutler, A. C.; Brittain, T.; Boyd, P. D. W. *J. Inorg. Biochem.* **1985**, *24*, 199. (d) Bulach, V.; Mandon, D.; Weiss, R. *Angew. Chem., Int. Ed. Engl.* **1991**, *30*, 572.

(27) (a) Nanthakumar, A.; Nasir, M. S.; Karlin, K. D.; Ravi, N.; Huynh, B. H. *J. Am. Chem. Soc.* **1992**, *114*, 6564. (b) After submission of this paper, Nanthakumar et al. reported the preparation (by a different method) of a heme–Cu bridged assembly with a linear Cu^{II}–O–Fe^{III} bridge and an antiferromagnetically coupled S = 2 ground state (J = –87 cm^{-1} in $H = -2JS_1S_2$): Nanthakumar, A.; Fox, S.; Murthy, N. N.; Karlin, K. D.; Ravi, N.; Huynh, B. H.; Orosz, R. D.; Day, E. P.; Hagen, K. S.; Blackburn, N. *J. Am. Chem. Soc.* **1993**, *115*, 8513.

(28) Lee, S. C.; Holm, R. H. *J. Am. Chem. Soc.* **1993**, *115*, 5833.

(29) Ciampolini, M.; Nardi, N. *Inorg. Chem.* **1966**, *5*, 41. (Me$_6$tren = tris((*N*,*N*-dimethylamino)ethyl)amine.)

(30) Dolphin, D. H.; Sams, J. R.; Tsin, T. B. *Inorg. Chem.* **1977**, *16*, 711. (OEP = octaethylporphyrinate(2–).)

(31) Cromer, D. T.; Waber, J. T. *International Tables for X-ray Crystallography*; Kynoch Press: Birmingham, England, 1974; Vol. IV.

of noncentrosymmetric **2** with the atom positions inverted through the origin was found to converge at a significantly lower R value; this enantiomorph was accepted as correct. Crystallographic data are provided in Table I.

All structures displayed some degree of disorder; if separate components of the disorder were resolvable, the occupancy factors of the individual orientations were refined with their sum constrained to unity, then fixed in the final refinements, unless otherwise indicated. Compound **1**: The two perchlorate counterions associated with molecule 1 were found to be disordered. One disordered perchlorate could be distinguished in two orientations and was treated accordingly; the disorder in the other perchlorate could not be resolved and is evident in the elongated anisotropic ellipsoids in the final structure. Compound **2**: The perchlorate anion was disordered across two orientations and was treated without difficulty. Monoclinic compound **3**: Molecule 2 displayed resolvable disorder in one ethyl arm orientation; in addition, terminal C/N atoms of one acetonitrile solvate molecule were scrambled and simply treated as carbons. Orthorhombic **3**: This structure is dominated by the crystallographic mirror symmetry imposed on a *nearly* mirror symmetric oxo-bridged cation.[32] The methyl group on Me_6tren and one ethyl arm on the OEP showed resolvable disorder. The orientation of the perchlorate counterion, located on a crystallographic inversion center, was determined, and occupancies were fixed at 0.5. Finally, residual electron density, corresponding to a highly disordered molecule, probably THF, was located accross a mirror plane in the lattice; isotropic thermal parameters were refined to absorb the density.

All non-hydrogen atoms were treated anisotropically, with the exception of the distinguishable disordered perchlorate atoms in **1**. Blocked matrix least-squares refinement was employed for **1** and monoclinic **3** owing to the number of parameters; full matrix least-squares refinements were used in all other cases. In the final stages of refinement, hydrogen atoms were placed on the Me_6tren ligand in **1** and **2** and on the OEP ligands in both forms of **3** at calculated positions 0.96 Å from, and with isotropic thermal parameters 1.2× those of, their parent carbon atoms. The high thermal motion of the Me_6tren ligand atoms in the structures of **3** precluded hydrogen atom placement at those sites. No hydrogens could be located for the aquo ligands in **1**. The final difference Fourier map of **2** revealed the hydrogen atom on the hydroxo ligand, as well as the lattice water hydrogen participating in hydrogen bond donation to the hydroxo, at reasonable positions; the other hydrogen on the lattice water could not be found. The disorder present in all of these structures accounted for multiple peaks of residual electron density, none greater than 1 $e^-/Å^3$, that were evident in final difference Fourier maps. Final R values are provided in Table I.[33]

Other Physical Measurements. Absorption spectra were determined with a Cary 219 spectrophotometer. EPR spectra were measured with the use of a Bruker ESP 300E spectrometer. ^1H NMR spectra were recorded on a Bruker AM500 instrument. Microprobe analyses were performed on crystalline samples by a Cameca MBX electron microprobe using a Tracor Northern TH-1310 wavelength-dispersive spectrometer with a TN-5502 EDS system and a stage automation system. The following standards were used: Fe metal, Cu metal, sodalite (Cl). Variable temperature magnetic susceptibility measurements were obtained on a Quantum Design MPMS SQUID magnetometer at the Tufts University Magnetometry Facility, using 10–25 mg of sample compressed in gelatin capsules. Magnetic data were corrected for diamagnetism: -450×10^{-6} emu/mol for H_2OEP[34] and Pascal's constants[35] for the remainder of the complex, giving -666×10^{-6} emu/mol as the correction for compound **3**.

Results and Discussion

Previous synthetic approaches have encompassed a considerable variety of putative or proven Fe–X–Cu bridge units, including X = imidazolate,[19] bipyrimidinyl,[20] Cl^-/Br^-,[21] OH^-/O^{2-},[21a,d,22] RCO_2^-,[23] N_3^-,[21c] CN^-,[21a,c,24] and enethiolate.[25] In other cases, the bridge was unidentified or the metals were not directly linked.[26] The minimum specifications for an acceptable as-isolated CcO site analogue can be summarized as (1) a structural requirement of a high-spin ($S = 5/2$) Fe(III) porphyrin, a N-ligated Cu(II) component, and a biologically probable bridge capable of effectively propagating superexchange, all arranged with proper orbital geometry to promote (2) an electronic requirement of strong antiferromagnetic interaction. To meet these criteria, the oxo-bridged heme–copper moiety—a plausible functional group for a reaction center that undergoes oxygenation chemistry—was chosen as the synthetic target.

Synthetic Analysis. The μ_2-oxo functionality,[36] M–O–M, is widely distributed across the transition series, being particularly familiar in Fe(III) chemistry.[37] In contrast, this group apprears rarely for Cu(II), its existence being largely inferred by reactivity arguments, with no structurally characterized examples extant.[38] Because of the lack of unfilled metal orbitals on Cu(II) (d^9) for π-acceptance from oxide, such a bridge is likely to be decidedly basic, much more so than the Fe(III) homologue, and reactive. No *proven* examples of the Fe–O–Cu unit exist (vide infra).

Several synthetic transformations, both redox and acid–base, are capable of generating oxo bridges.[36] Two dissimilar methodological themes may be discerned in the relationship of these transforms to the construction of bridged assemblies: *self-assembly* and *directed synthesis*. Most syntheses of oxo bridges rely on self-assembly to achieve the functional group, with the oxo synthon present as a component extrinsic to both metals. While this is of little consequence for a symmetric bridged dimer, its utility for synthesis of an asymmetric Fe–O–Cu assembly is limited by the probable formation of mixtures of products including the notably stable Fe^{III}–O–Fe^{III} bridged complex.[39]

The methodological alternative to self-assembly is directed synthesis, where the bridge synthon is intrinsic to one of the metal complexes, remaining bound at that site through the reaction course. Directed synthesis potentially offers a higher degree of control over product identity and yield than self-assembly. It has been successfully employed in attaining heterodimeric oxo bridges on several occasions[36,40] via redox reaction 2, an incomplete oxo-transfer.[41] With respect to iron and copper, this specific transformation is complicated by the absence of terminal oxo on copper and the instability of ferryl porphyrin as a reagent. The pertinent reaction 3 has been briefly reported,[22b] but the formulation of the product has been questioned.[42]

(32) Refinement was attempted in the noncentrosymmetric space group in an effort to resolve the disorder; this choice was rejected when the refinement was found to be unstable. Given the dominant symmetric nature of the molecule, the centrosymmetric choice is crystallographically proper. (a) Bauer, W. H.; Tillmanns, E. *Acta Crystallogr.* **1986**, *B42*, 95. (b) Marsh, R. E. *Acta Crystallogr.* **1986**, *B42*, 193.

(33) See paragraph at the end of this article concerning supplementary material.

(34) Sutton, T. P. G.; Hambright, P.; Thorpe, A. N.; Quoc, N. *Inorg. Chim. Acta* **1992**, *195*, 131.

(35) Carlin, R. L. *Magnetochemistry*; Springer-Verlag: Berlin, 1986; p 4.

(36) West, B. O. *Polyhedron* **1989**, *8*, 219. This account gives a general overview on oxo-bridged metal complexes, including a comprehensive and relevant section devoted to heteronuclear oxo-bridged species.

(37) Kurtz, D. M. *Chem. Rev.* **1990**, *90*, 585.

(38) Two complexes are claimed as possessing the Cu–O–Cu moiety: (a) Chaudhuri, P.; Ventur, D.; Wieghardt, K.; Peters, E.-M.; Peters, K.; Simon, A. *Angew. Chem., Int. Ed. Engl.* **1985**, *24*, 57. Two "tautomeric" complexes with the cores $[Cu_2(\mu\text{-}O)(\mu\text{-}OH_2)]^{2+}$ and $[Cu_2(\mu\text{-}OH)_2]^{2+}$ are described; the published observations, however, are consistent with chloride contamination in the putative oxo-bridged species, as in the so-called "bond stretch" isomers: Parkin, G. *Chem. Rev.* **1993**, *93*, 887. (b) Albert, C. F.; Healy, P. C.; Kildea, J. D.; Raston, C. L.; Skelton, B. W.; White, A. H. *Inorg. Chem.* **1989**, *28*, 1300. A hexanuclear Cu(I) complex is described with a Cu–O–Cu bridge; refinement of the putative oxygen atom was problematic.

(39) However, self-assembly has been effectively employed in cases where the problem of mixtures has been mitigated by solubility differences: (a) Hotzelmann, R.; Wieghardt, K.; Ensling, J.; Romstedt, H.; Gütlich, P.; Bill, E.; Flörke, U.; Haupt, H.-J. *J. Am. Chem. Soc.* **1992**, *114*, 9470. (b) Hotzelmann, R.; Wieghardt, K.; Flörke, U.; Haupt, H.-J.; Weatherburn, D. C.; Bonvoisin, J.; Blondin, G.; Girerd, J.-J. *J. Am. Chem. Soc.* **1992**, *114*, 1681. (c) Holman, T. R.; Andersen, K. A.; Anderson, O. P.; Hendrich, M. P.; Juarez-Garcia, C.; Münck, E.; Que, L., Jr. *Angew. Chem., Int. Ed. Engl.* **1990**, *29*, 921.

(40) Selected structurally characterized examples follow. (a) Fe^{III}–O–Ru^{IV}–O–Fe^{III}: Schultz, L. D.; Fallon, G. D.; Moubaraki, B.; Murray, K. S.; West, B. O. *J. Chem. Soc., Chem. Commun.* **1992**, 971. (b) Fe^{III}–O–Cr^{III}: Liston, D. L.; Kennedy, B. J.; Murray, K. S.; West, B. O. *Inorg. Chem.* **1985**, *24*, 1561.

(41) Holm, R. H. *Chem. Rev.* **1987**, *87*, 1401.

(42) TPP = tetraphenylporphyrinate(2–). L = a pyridine/imidazole-derived pentadentate ligand. Gupta et al.[19f] have observed that the Mössbauer parameters of the product are more consistent with a low-spin bis(imidazole) Fe(III) porphyrin formulation.

$$M_A{}^m{=}O + M_B{}^n \rightarrow M_A{}^{m-1}\text{–}O\text{–}M_B{}^{n+1} \quad (2)$$

$$(TPP)Fe^{IV}{=}O + [Cu^{I}(L)]^+ \rightarrow [(TPP)Fe^{III}\text{–}O\text{–}Cu^{II}(L)]^+ \quad (3)$$

A further synthetic option involves the construction of an assembly in which both metals are tethered to a shared chelating ligand. The binucleating ligand provides a void between the metal sites where the desired ligand X may be inserted to afford a bridge M_A–X–M_B. This tactic has been employed in CcO analogue synthesis on several occasions via iron porphyrins elaborated with covalently attached ligands for copper.[21,22a,c,26d]

We have investigated the directed acid–base reaction 4, in which L is labile ligand and B is a suitable base. Although this

$$M_A\text{–}OH + M_B\text{–}L + B \rightarrow M_A\text{–}O\text{–}M_B + L^- + BH^+ \quad (4)$$

reaction is mechanistically equivalent to well-known hydrolytic self-assembly routes to μ-oxo dimers,[36] we are unaware of any previous application in the synthesis of asymmetric assemblies, a factor attributed to the rare occurrence of terminal hydroxide as a ligand. In iron porphyrin chemistry, for example, terminal hydroxide has only a brief existence unless the porphyrin is derivatized to prevent Fe^{III}–O–Fe^{III} formation,[43] the degenerate form of reaction 4. For Cu(II) complexes, related self-reactions resulting in the stable $[Cu_2(\mu\text{-}OH)_2]^{2+}$ [13] or the less soluble $[Cu_2(\mu\text{-}OH)]^{3+}$ dimers[44] are problematic for the persistence of terminal hydroxide ligation. Structurally characterized examples of terminal $[Cu\text{–}OH]^+$ have been sporadically reported;[45] of the six known structures, four are probably misformulated on the basis of bond distances (vide infra), with the putative hydroxo actually an aquo ligand, and the other two are uncertain or unsuitable for the purpose at hand. It remains possible, however, that modification of the ligand environment at copper could stabilize $[Cu\text{–}OH]^+$, in the same way it does for the $[Fe\text{–}OH]^{2+}$ in porphyrins[43] and the terminal $[Zn\text{–}OH]^+$ group.[46] From these considerations, $[Cu\text{–}OH]^+$ was selected as the intermediate synthon for the oxo-bridged assembly.

Syntheses and Structures. Reactions 5–7 involving compounds **1**–**4** are set out in Scheme I.

(a) $[Cu(Me_6tren)(OH_2)]^{2+}$ ($[1]^{2+}$). Reaction 5 yields a blue fused crystalline mass, originally formulated, after recrystallization from nitromethane, as $\{Cu(Me_6tren)(OClO_3)\}(ClO_4)$ on the basis of Cu and N analyses.[29] In this work, X-ray diffraction of the initial crystalline product has shown it to be the *aquo* complex salt $[Cu(Me_6tren)(OH_2)](ClO_4)_2$.

Scheme I. Synthesis of Heme–Cu(II) Bridged Assembly

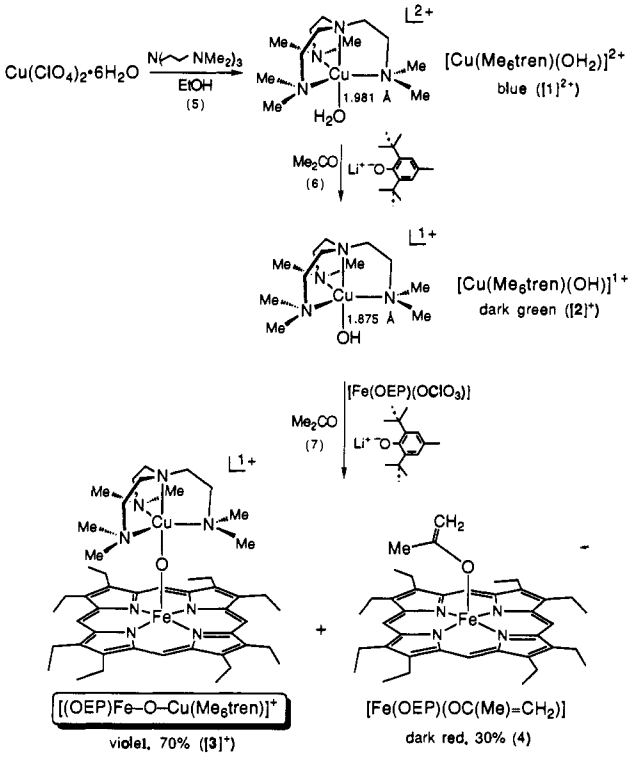

Table II. Selected Interatomic Distances (Å) and Angles (deg) in $[Cu(Me_6tren)(OH_2)](ClO_4)_2$ (**1**) and $[Cu(Me_6tren)(OH)](ClO_4)\cdot H_2O$ (**2**)[a]

	1, molecule 1	**1**, molecule 2	**2**
Cu(1)–O(1)	1.973(4)	1.990(4)	1.875(2)
Cu(1)–N(1)	2.131(5)	2.096(4)	2.163(3)
Cu(1)–N(2)	2.123(5)	2.124(4)	2.161(3)
Cu(1)–N(3)	2.149(4)	2.160(4)	2.189(3)
Cu(1)–N(4)	2.014(5)	1.996(4)	2.049(3)
Cu(1)–Ct_{Me}	0.76	0.78	0.71
O(1)–Cu(1)–N(1)	95.7(2)	92.8(2)	96.6(1)
O(1)–Cu(1)–N(2)	93.6(2)	94.4(2)	92.1(1)
O(1)–Cu(1)–N(3)	92.7(2)	94.3(2)	98.1(1)
O(1)–Cu(1)–N(4)	178.0(2)	178.3(2)	176.3(1)
N(1)–Cu(1)–N(2)	120.1(2)	122.0(2)	119.6(1)
N(1)–Cu(1)–N(3)	119.2(2)	119.0(2)	117.7(1)
N(1)–Cu(1)–N(4)	86.1(2)	85.6(2)	84.7(1)
N(2)–Cu(1)–N(3)	119.2(2)	117.8(2)	119.9(2)
N(2)–Cu(1)–N(4)	86.1(3)	86.9(2)	84.2(1)
N(3)–Cu(1)–N(4)	85.7(2)	86.2(2)	84.4(1)

[a] Atom labels of **1**, molecule 2, correspond as Cu(2→1), O(2,31,43→1,13,17), N(1...4→5...8); see Figure 2. Ct_{Me} is the centroid of the three bottom protruding methyl carbon atoms.

Compound **1** crystallizes in a centrosymmetric monoclinic unit cell with two independent molecules, shown in Figure 2, in the asymmetric unit; selected metric data are contained in Table II. The two molecules are structurally equivalent, differing only in the counterion disorder and consequent higher overall thermal motion associated with molecule 1. Some nine isostructural complexes $[M(Me_6tren)X]^+$ have been structurally characterized,[47] including $[Cu(Me_6tren)Br]^+$.[47b] As in prior structures, tetradentate Me_6tren coordinates in a tripodal manner, enforcing a trigonal bipyramidal geometry at the metal in complex $[1]^{2+}$; each arm of the ligand forms a puckered five-membered chelate ring, with the ring conformations synchronized to impart an axial

(43) (a) Woon, T. C.; Shirazi, A.; Bruice, T. C. *Inorg. Chem.* **1986**, *25*, 3845. (b) More, K. M.; Eaton, G. R.; Eaton, S. S. *Inorg. Chem.* **1985**, *24*, 3698. (c) Fielding, L.; Eaton, G. R.; Eaton, S. S. *Inorg. Chem.* **1985**, *24*, 2309.

(44) (a) Castro, I.; Faus, J.; Julve, M.; Lloret, F.; Verdaguer, M.; Kahn, O.; Jeannin, S.; Jeannin, Y.; Vaisserman, J. *J. Chem. Soc., Dalton Trans.* **1990**, 2207 and references therein. (b) Spodine, E.; Manzur, J.; Garland, M. T.; Kiwi, M.; Peña, O.; Grandjean, D.; Toupet, L. *J. Chem. Soc., Dalton Trans.* **1991**, 365 and references therein.

(45) (a) Klein, C. L.; Stevens, E. D.; O'Connor, C. J.; Majeste, R. J.; Trefonas, L. M. *Inorg. Chim. Acta* **1983**, *70*, 151. Cu–OH = 2.46 Å. (b) Goodgame, D. M. L.; Williams, D. J.; Winpenny, R. E. P. *Polyhedron* **1989**, *8*, 1531. Cu–OH = 2.33, 2.36 Å (two structures). (c) Mathews, I. L.; Sudhakara Rao, S. P.; Nethaji, M. *Polyhedron* **1992**, *11*, 1397. Cu–OH = 2.22 Å. (d) Amirov, G. T.; Abdullaev, G. K.; Mamedov, Kh. S. *J. Struct. Chem.* **1975**, *16*, 471. The complex displays two trans ligands at a distance (1.91 Å) consistent with Cu^{II}–OH units; however, the *R* value is exceptionally high (16%) for a structure with only seven non-hydrogen atoms in the asymmetric unit. (e) Tamura, H.; Ogawa, K.; Mori, W. *J. Crystallogr. Spectrosc. Res.* **1989**, *19*, 203. The structure is a complex polynuclear hydrogen-bonded network of lattice and coordinated water molecules; the assignment of terminal hydroxide to bonds with Cu^{II}–O = 1.92–2.05 Å is plausible.

(46) (a) Alsfasser, R.; Trofimenko, S.; Looney, A.; Parkin, G.; Vahrenkamp, H. *Inorg. Chem.* **1991**, *30*, 4098. (b) Looney, A.; Han, R.; McNeill, K.; Parkin, G. *J. Am. Chem. Soc.* **1993**, *115*, 4690.

(47) (a) Di Vaira, M.; Orioli, P. L. *Inorg. Chem.* **1967**, *6*, 955. (b) Di Vaira, M.; Orioli, P. L. *Acta Crystallogr., Sect. B* **1968**, *24* 595. (c) Di Vaira, M.; Orioli, P. L. *Acta Crystallogr., Sect. B* **1968**, *24*, 1269. (d) Oriolo, P. L.; Ciampolini, M. *J. Chem. Soc., Chem. Commun.* **1972**, 1280. (e) Dapporto, P.; Gatteschi, D. *Cryst. Struct. Commun.* **1973**, *2*, 137. (f) Colpas, G. J.; Kumar, M.; Day, R. O.; Maroney, M. J. *Inorg. Chem.* **1990**, *29*, 4779.

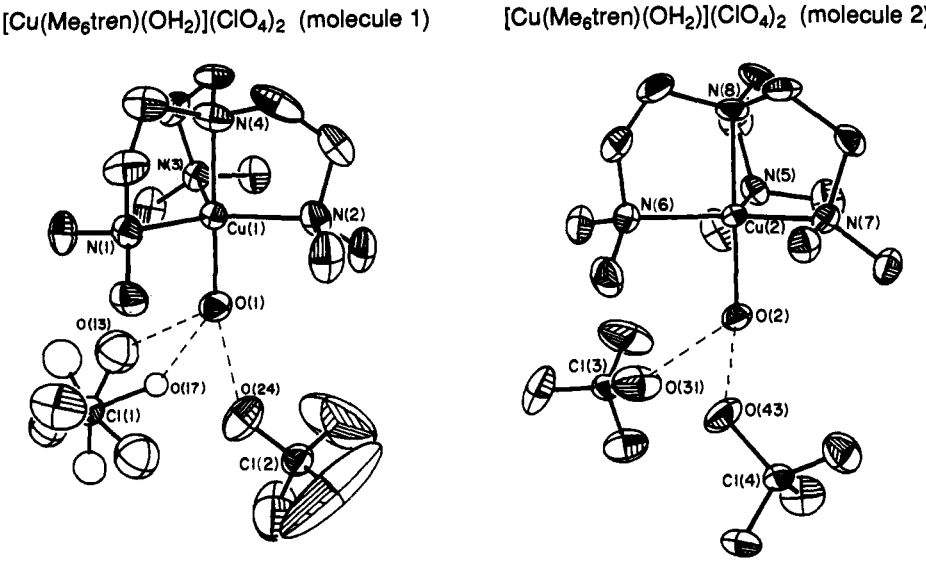

Figure 2. Structures of the two inequivalent molecules of $[Cu(Me_6tren)(OH_2)](ClO_4)_2$, with the atom-labeling schemes and 50% probability ellipsoids. Alternate positions of disordered atoms are shown with open circles and bonds; isotropically refined atoms are shown without shaded segments.

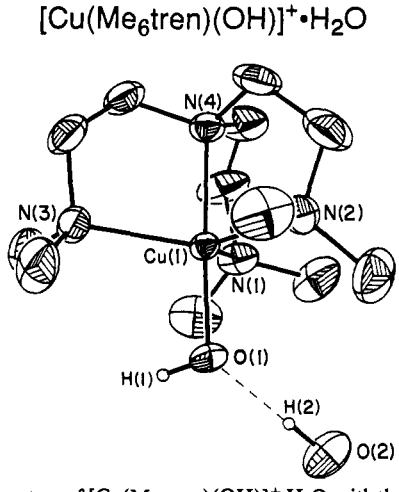

Figure 3. Structure of $[Cu(Me_6tren)(OH)]^+ \cdot H_2O$, with the atom-labeling scheme and 50% probability ellipsoids.

C_3 twist to the bound ligand. The chelate conformation forces one methyl group from each arm to project downward, the three groups forming a plane >0.7 Å below the copper atom; this provides a steric barrier that may hinder self-dimerization. The axial Cu–N distance is significantly shorter than the equatorial distances, well-precedented behavior for trigonal bipyramidal Cu(II).[47b,48] The remaining coordination site is axial and occupied by water; on the basis of inter-oxygen distances involving O(1,2)[33] that occur in the range 2.56(2)–2.88(1) Å, the aquo ligand also participates in hydrogen-bonding with two perchlorate anions.

(b) $[Cu(Me_6tren)(OH)]^+$ ($[2]^+$). Treatment of aquo complex $[1]^{2+}$ with 1 equiv of KOH under a variety of conditions gave complex reaction mixtures consisting of viscous residues and glassy solids. However, on several occasions, blue crystals were obtained from the complex product mixture and were identified as $[Cu(Me_6tren)(OH)](ClO_4)\cdot H_2O$ (**2**) by X-ray diffraction. The structure of compound **2** is set out in Figure 3; metric data are collected in Table II. The $Cu(Me_6tren)^{2+}$ portions of complexes $[1]^{2+}$ and $[2]^+$ are isostructural and essentially isometric. The only significant structural difference is the Cu–O bond length of 1.875(2) Å in the latter, comparable with the Cu^{II}–O separation in terminal alkoxides (1.90(3)Å)[49] and shorter by 0.10–0.12 Å than that in $[1]^{2+}$. This feature together with the presence of one anion establishes the existence of an axial hydroxide ligand. The terminal hydroxide participates as a hydrogen-bond acceptor from a lattice water molecule. The donor hydrogen atom and the hydrogen atom belonging to the terminal hydroxide were located at reasonable positions on the final difference Fourier map; in the hydrogen bond, O(1)···O(2) = 2.697(4) Å, O(1)···H(2) = 1.80 Å, and O(2)–H(2) = 0.90 Å. Note the large differences between the Cu–O bond length in $[2]^+$ and those in certain claimed examples of the Cu^{II}–OH unit.[45] In previous work, we have shown that long Cu^{II}–OH distances do not occur for bridging hydroxide; thus a long distance for terminal hydroxide is highly unlikely.[28]

Despite multiple attempts with different bases under a variety of conditions, both protic and rigorously aprotic, a useful synthesis of **2** was not achieved. The reaction appears to produce several soluble copper species in addition to, and probably in equilibrium with, $[2]^+$. Nevertheless, the structural characterization of **2** demonstrates that terminal hydroxide is compatible with the $[Cu(Me_6tren)]^{2+}$ environment.

(c) $[(OEP)Fe\text{-}O\text{-}Cu(Me_6tren)]^+$ ($[3]^+$). (i) Synthesis. Reaction 4 was reduced to practice by means of reactions 6 and 7 in Scheme I, which afforded the desired bridged assembly $[3]^+$. Given the inability to isolate bulk quantities of $[2]^+$ in any form, it was necessary to generate this complex as an intermediate in solution. Treatment of $[1]^{2+}$ with 2 equiv of the hindered base lithium 2,6-di-*tert*-butyl-4-methylphenolate (LiOPh*) in acetone resulted in a dark green solution containing $[2]^+$. Addition of $[Fe(OEP)(OClO_3)]$,[30] whose axial ligand is decidedly labile, afforded a purple solution from which was isolated violet microcrystals of the desired product $[(OEP)Fe\text{–}O\text{–}Cu(Me_6tren)](ClO_4)$ (**3**), typically in 70% yield. This compound is soluble and stable under aprotic conditions in a variety of solvents including THF, dichloromethane, acetone, acetonitrile, and DMF.

Both solvent and base influence the outcome of reaction 7. In acetone, the coupling reaction generates, in addition to $[3]^+$, a high-spin Fe(III) porphyrin coproduct with equally intense methylene resonances at δ 28.4 and 31.9 and a further methyl signal at δ 4.80. This species can be independently generated by the addition of strong base to $[Fe(OEP)(OClO_3)]$ in acetone and is believed to be the previously unknown enolate complex $[Fe(OEP)OC(Me)=CH_2]$ (**4**). Based on the relative intensities of NMR signals, the mol ratio $[3]^+$:**4** ≈ 2:1 is typically generated

(48) Bernal, I.; Korp, J. D.; Schlemper, E. O.; Hussain, M. S. *Polyhedron* **1982**, *1*, 365 and references therein.

(49) Orpen, A. G.; Brammer, L.; Allen, F. H.; Kennard, O.; Watson, D. G.; Taylor, R. *J. Chem. Soc., Dalton Trans.* **1989**, Supplement, S1.

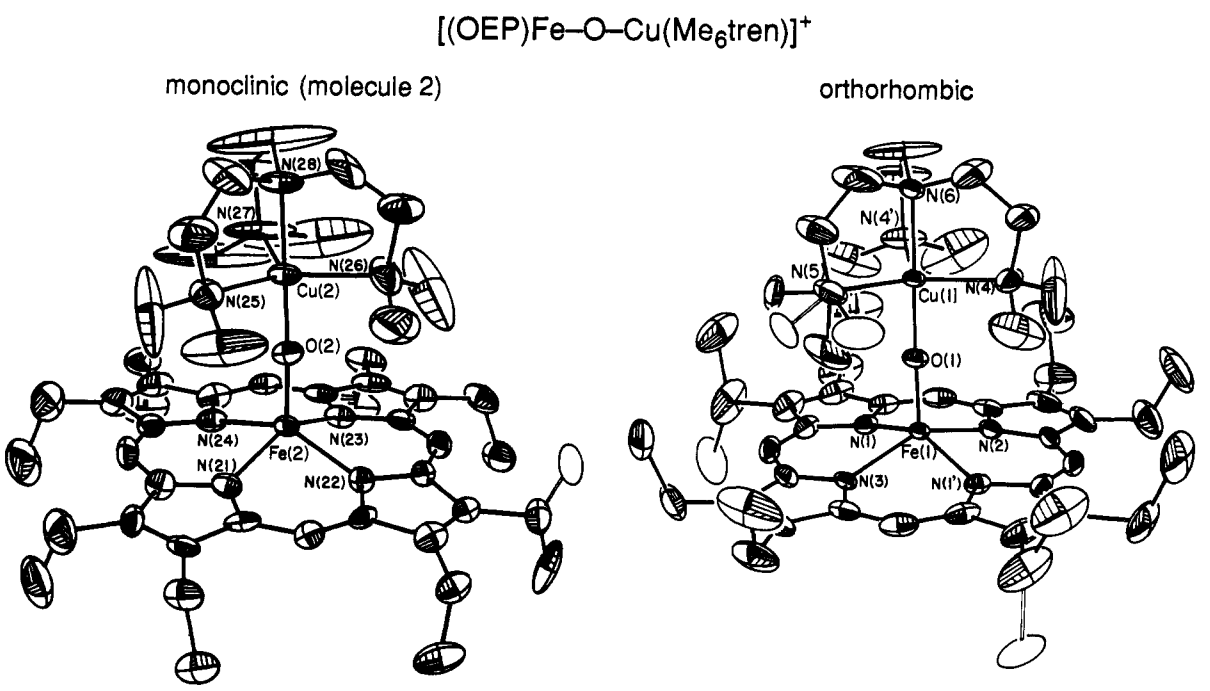

Figure 4. Structures of [(OEP)Fe–O–Cu(Me_6tren)]$^+$ in two different crystalline forms, showing the atom-labeling schemes and 50% probability ellipsoids: left, molecule 2 in the monoclinic form; right, orthorhombic form. A depiction of molecule 1 in the monoclinic form has been presented.[28] Disordered atoms are represented as in Figure 2.

Table III. Selected Interatomic Distances (Å) and Angles (deg) in [(OEP)Fe–O–Cu(Me_6tren)](ClO_4), MeCN Solvate (3·MeCN) and THF Solvate (3·THF)[a]

	3·MeCN, x = 1	3·MeCN, x = 2	3·THF
Fe(x)···Cu(x)	3.570(1)	3.572(1)	3.575(1)
Fe(x)–O(x)	1.745(4)	1.743(4)	1.747(7)
Fe(x)–N(x1)	2.104(6)	2.109(6)	2.099(4)
Fe(x)–N(x2)	2.123(5)	2.103(6)	2.098(5)
Fe(x)–N(x3)	2.110(5)	2.114(5)	2.108(5)
Fe(x)–N(x4)	2.101(5)	2.124(6)	
Fe(x)–N_{mean}	2.11(1)	2.113(9)	2.101(5)
Fe(x)···Ct_{por}	0.67	0.67	0.62
Ct_{por}···N_{mean}	2.03	2.03	2.03
Cu(x)–O(x)	1.829(4)	1.830(4)	1.828(4)
Cu(x)–N(x5)	2.151(7)	2.157(6)	2.166(7)
Cu(x)–N(x6)	2.108(7)	2.179(7)	2.024(5)
Cu(x)–N(x7)	2.149(7)	2.120(6)	2.158(5)
Cu(x)–N(x8)	2.064(6)	2.045(5)	
Cu(x)–O(x)–Fe(x)	175.2(3)	176.6(3)	178.2(3)
O(x)–Fe(x)–N(x1)	106.7(2)	104.3(2)	105.0(1)
O(x)–Fe(x)–N(x2)	106.8(2)	106.1(2)	106.9(2)
O(x)–Fe(x)–N(x3)	104.9(2)	107.7(2)	104.6(2)
O(x)–Fe(x)–N(x4)	104.9(2)	105.7(2)	
N(x1)–Fe(x)–N(x2)	85.8(2)	85.6(2)	86.2(1)
N(x1)–Fe(x)–N(x3)	148.5(2)	147.9(2)	85.8(1)
N(x1)–Fe(x)–N(x4)	85.5(2)	85.8(2)	150.1(2)
N(x2)–Fe(x)–N(x3)	85.6(2)	85.6(2)	148.5(2)
N(x2)–Fe(x)–N(x4)	148.2(2)	148.2(2)	
N(x3)–Fe(x)–N(x4)	86.0(2)	85.5(2)	
O(x)–Cu(x)–N(x5)	95.5(2)	97.0(2)	95.6(2)
O(x)–Cu(x)–N(x6)	94.6(2)	94.7(2)	179.6(2)
O(x)–Cu(x)–N(x7)	95.5(2)	94.8(2)	95.7(1)
O(x)–Cu(x)–N(x8)	178.5(3)	179.3(2)	
N(x5)–Cu(x)–N(x6)	118.2(4)	117.5(3)	84.0(2)
N(x5)–Cu(x)–N(x7)	115.9(3)	118.3(4)	119.9(2)
N(x5)–Cu(x)–N(x8)	83.4(3)	83.7(2)	
N(x6)–Cu(x)–N(x7)	123.7(4)	121.5(4)	84.5(1)
N(x6)–Cu(x)–N(x8)	85.0(3)	85.3(3)	
N(x7)–Cu(x)–N(x8)	85.9(3)	84.5(2)	117.2(3)

[a] Atom labels of 3·THF correspond as Fe(x→1), Cu(x→1), O(x→1), N(x1,x2,x3,x4,x5,x6,x7,x8→1,2,3,1′,5,6,4,4′); see Figure 3. Ct_{por} is the centroid of the 24-atom (C, N) porphyrin core.

in actone solution. In DMF, [3]$^+$ is also formed together with the coproduct [Fe(OEP)]$_2$O, readily identified by its ^{1}H NMR spectrum,[50] which partially precipitates from the reaction mixture. In acetonitrile, the reaction is marked by minority formation of [3]$^+$ and copious precipitation of [Fe(OEP)]$_2$O.

The effect of the deprotonating agent was also explored in an effort to maximize the yield of [3]$^+$ in acetone reaction mixtures. Use of the hindered phosphazene base *tert*-butylimino-tris-(dimethylamino)phosphorane ($pK_{BH^+} \approx 26.5$[51])produced the bridged assembly and the enolate coproduct in roughly equal amounts. The more basic LiOPh* ($pK_{BH} \approx 30$[51]) favored the synthesis of [3]$^+$ to enolate by approximately 2:1. (Ion pairing and aggregation of the lithium salt may reduce the effective basicity of the anion in a low-dielectric solvent.) The use of the moderately basic tertiary amine 1,2,2,6,6-pentamethylpiperidine (PMP) ($pK_{BH^+} \approx 18.6$[51]) led to essentially *quantitative* production of the bridged assembly **3**, with no other NMR-active porphyrin species present at a significant level. The lower dielectric and weaker coordinating ability of acetone may disfavor the hydroxide transfer to iron; this, in concert with a moderate base incapable of rapidly generating enolate on ferric porphyrin, may explain the clean assembly of **3** in the PMP/acetone system.

The choice of synthetic procedure was ultimately determined by its utility in isolating bulk quantities of pure **3**. The conjugate acid–perchlorate salts of neutral bases were found to complicate product isolation by cocrystallizing with **3**; in addition, the bridged assembly appears unstable to workup in the presence of tertiary ammonium cations, with [Fe(OEP)(OC(Me)=CH_2)] as the final isolated product. Thus, LiOPh* was employed in the bulk synthesis of **3** in acceptable yield, with sideproducts ($LiClO_4$ and HOPh*) easily removed by dissolution in ether.

(ii) Structure. Conclusive identification of **3** was obtained by X-ray diffraction analysis of two separate crystal forms, proving the unprecedented Fe–O–Cu unit as the bridge between the square pyramidal iron porphyrin and trigonal bipyramidal copper. Structures are shown in Figure 4; selected distance and angle data are compiled in Table III. Crystals grown from ether diffusion into acetonitrile solutions of **3** contain two independent

(50) La Mar, G. N.; Eaton, G. R.; Holm, R. H.; Walker, F. A. *J. Am. Chem. Soc.* **1973**, *95*, 63.

(51) Schwesinger, R. *Nachr. Chem., Tech. Lab.* **1990**, *38*, 1214. The pK_{BH^+} values refer to acetonitrile solutions.

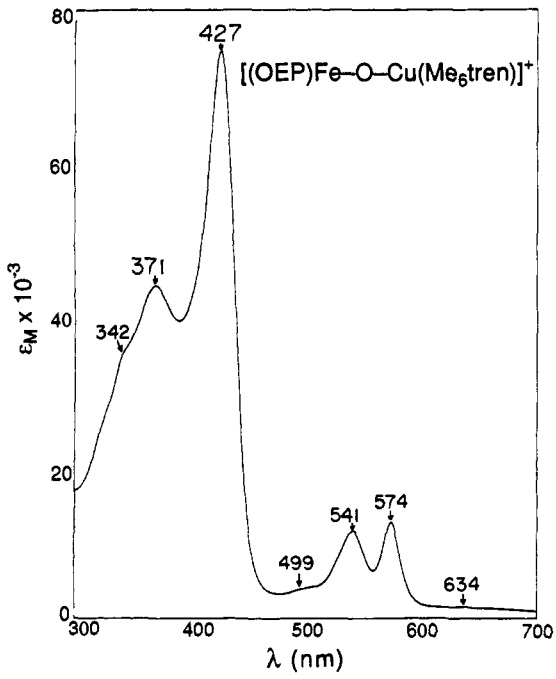

Figure 5. UV/visible absorption spectrum of [(OEP)Fe–O–Cu(Me$_6$-tren)]$^+$ in dichloromethane solution; band maxima are indicated.

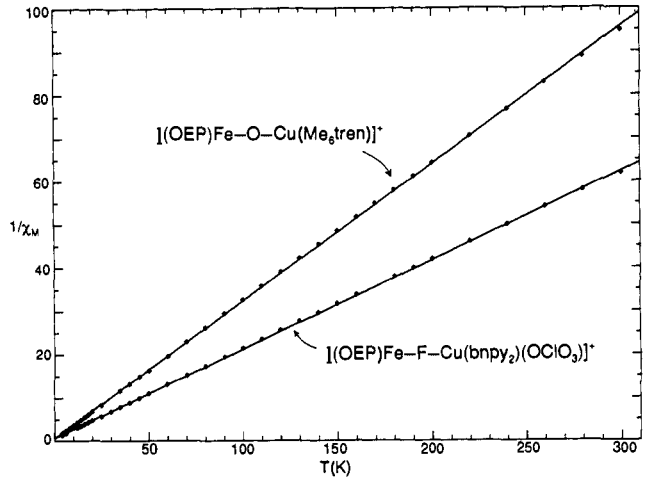

Figure 6. Temperature dependence of the reciprocal magnetic susceptibilities of [(OEP)Fe–O–Cu(Me$_6$tren)]$^+$ and [(OEP)Fe–F–Cu(bnpy$_2$)-(OClO$_3$)]$^+$ at 4.2-300 K. The solid lines are linear least-squares fits to the data (see text).

molecules in the asymmetric unit of a centrosymmetric monoclinic cell; the independent molecules differ simply in the relative orientation of porphyrin ethyl arms. Orthorhombic crystals were obtained from the layering of ether onto a THF solution; [**3**]$^+$ resides on a crystallographic mirror plane in this form, with minor ligand disorder as a result.

All three independent cations of **3** possess essentially identical core dimensions. The Fe–N bond distances and the relatively large displacements of the Fe atoms from the porphyrin core are consistent with those of five-coordinate high-spin mononuclear and μ-oxo Fe(III) porphyrins.[52] The Cu–N distances are also normal and comparable, with a striking degree of thermal motion in all structures; ellipsoids are elongated in the trigonal plane, and N–C–C–N chelate rings are nearly planar instead of puckered. The origin of this disorder is attributable to the close interligand contact enforced by the oxo bridge. Given the Fe···Cu separation (3.6 Å), rough calculation of distances between the porphyrin

(52) (a) Scheidt, W. R.; Lee, Y. J. *Struct. Bonding (Berlin)* **1987**, *64*, 1. (b) Scheidt, W. R.; Reed, C. A. *Chem. Rev.* **1981**, *81*, 543.

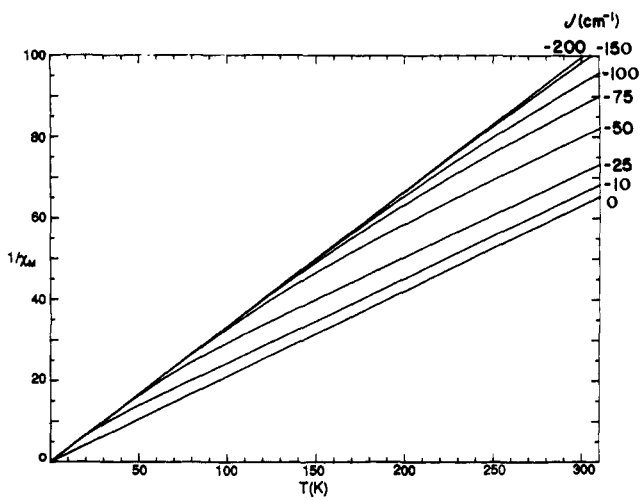

Figure 7. Temperature dependence of the reciprocal magnetic susceptibility of antiferromagnetically coupled $S = 5/2$ and $1/2$ centers with J in the range -10 to -200 cm^{-1} and $J = 0$.

plane and an idealized Me$_6$tren ligand (using the structure of [**2**]$^+$, with a projecting methyl carbon atom plane 0.7 Å below the copper atom) shows a contact distance of 3.5 Å, somewhat shorter than the van der Waals minimum at 3.75 Å.[53]

The most significant structural feature is the unsupported oxo bridge. Both the bridge angles Fe–O–Cu, with a mean value of 176.6°, and the displacements Fe···Ct$_{por}$ = 0.62–0.67 Å presumably arise from the interligand contact noted above. The mean Fe–O distance of 1.745 Å is indistinguishable from the corresponding value of 1.757 Å in [Fe(OEP)]$_2$O.[54] While no structurally proven examples exist of the [Cu$_2$(μ-O)]$^{2+}$ bridge, the mean Cu–O distance of 1.829 Å is comparable to the Cu–OH distance in [**2**]$^+$. While the composition of compound **3** eliminates a monoanionic bridge atom, we also note that the values Fe–O = 1.94 Å and Fe–O–Fe = 146.2° for [Fe(OEP)$_2$(OH)]$^+$ remove any possibility of a hydroxide bridge in [**3**]$^+$. Because the metric parameters of the bridge are practically invariant over three different crystalline environments, we take these to be intrinsic molecular properties.

Electronic Properties of the Bridged Assembly. The porphyrin-dominated UV/visible absorption spectrum of [**3**]$^+$ in dichloromethane solution, shown in Figure 5, is presented primarily for characterization purposes. The spectrum is distinctive and is quite different from that of [Fe(OEP)]$_2$O, whose Soret band is 385 nm (CH$_2$Cl$_2$).[54] An increase in negative charge has been empirically correlated with a decrease in Soret transition energies of Zn(TPP)L species.[55] In the present case, this interpretation is consistent with our expectation of a weaker Cu(II) affinity for the bridging oxo atom as compared with Fe(III).

Other electronic properties of [**3**]$^+$ are summarized in Table IV. The Mössbauer spectrum of polycrystalline **3** at 4.2 K consists of a single quadrupole doublet whose parameters serve to identify high-spin Fe(III),[56] in agreement with the structural data. The magnetic susceptibility behavior of **3** is well described by the Curie–Weiss law $\chi^M = C/(T - \theta)$. As shown in Figure 6, the dependence of the inverse molar susceptibility with temperature is nearly linear, with only very slight curvature over the complete temperature range (4-300 K). The linear least-squares fit of the full data set yields the parameters in Table IV; for an $S = 2$ system with $g = 2$, the Curie constant $C = 3$ emu K/mol. The deviation of C from this value is potentially attributable to spin–

(53) van der Waals radii: –CH$_3$, 1.95 Å; aromatic carbon atom, 1.80 Å. McCammon, A.; Wolynes, P. G.; Karplus, M. *Biochemistry* **1979**, *18*, 927.

(54) Scheidt, W. R.; Cheng, B.; Safo, M. K.; Cukiernik, F.; Marchon, J.-C.; Debrunner, P. G. *J. Am. Chem. Soc.* **1992**, *114*, 4420.

(55) Nappa, M.; Valentine, J. S. *J. Am. Chem. Soc.* **1978**, *100*, 5075.

(56) Sams, J. R.; Tsin, T. B. In *The Porphyrins*; Dolphin, D.; Ed.; Academic Press: New York, 1979; Vol. IV, Part B, Chapter 9.

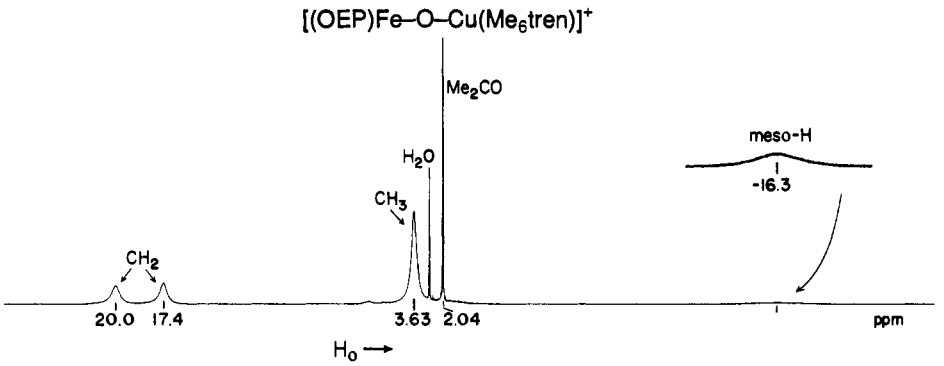

Figure 8. ^{1}H NMR spectrum of [(OEP)Fe–O–Cu(Me$_6$tren)]$^+$ in acetone-d_6 (292 K); signal assignments are indicated.

Table IV. Electronic Properties of [(OEP)Fe–O–Cu(Me$_6$tren)]$^+$

δ (mm/s)	0.48[a,b]
ΔE_Q (mm/s)	1.20[a,b]
C (emu K/mol)	3.15
θ (K)	2.03
μ_{eff} (μ_B)	5.03
$(\Delta H/H)_{iso}$ (ppm)[c,d]	−15.8, −13.2 (CH_2); −1.14 (CH_3), 26.6 (*meso*-H)

[a] 4.2 K. [b] Comparative data for bacterial and mammalian CCO[10]: δ = 0.41 mm/s, ΔE_Q = 1.1 mm/s (4.2 K). [c] 298 K. [d] Comparative CH_2 (OEP) shifts (ppm, 298 K): [Fe(OEP)(OC(Me)=CH_2)], −27.7, −24.2 (Me_2CO); [Fe(OEP)(OMe)], −28.5 (Me_2CO); −29.3, −26.4 (CD_2Cl_2); −28.2, −23.5 (C_6D_6). Resonances of the Me$_6$tren ligand are very broad and poorly defined.

orbit coupling effects. The magnetic behavior of coupled S = 5/2 and 1/2 spin systems can be described by eq 8,[57] where x = J/kT, J is the coupling constant ($H = -2JS_1S_2$), and the other symbols have their usual meanings. A plot of theoretical sus-

$$\chi^M = \frac{g^2\mu_B{}^2N}{kT}\left[\frac{10 + 28e^{6x}}{5 + 7e^{6x}}\right] \qquad (8)$$

ceptibility curves ($1/\chi^M$ vs T) as a function of $-J$ is presented in Figure 7;[58] magnitudes of $-J$ less than 200 cm^{-1} cause deviation from linearity in the temperature range of interest. The data for **3** show slight curvature when inspected by a difference plot vs the linear fit; however, the origin of this curvature, whether inherent to the compound or external from systematic error in the measurement technique, is unclear. Other potential sources of curvature include an incorrect estimate of diamagnetic correction, the presence of temperature-independent paramagnetism, or systematic instrumental response variations with temperature. *Nevertheless, the susceptibility data firmly establish compound 3 as a tightly coupled S = 2 system, the first such example in CcO analogue chemistry.* From Figure 7, we *estimate* that J occurs in the interval of −150 to −200 cm^{-1}. The most recent magnetic study of oxidized CcO has confirmed S = 2 paramagnetism, with $-J \geq 50$ cm^{-1}[19c]

The magnetic behavior of [**3**]$^+$ may be contrasted with that of the binuclear assembly [(OEP)Fe–F–Cu(bnpy$_2$)(OClO$_3$)](PF$_6$), which provides the closest available comparison. Here fluoride bridges five-coordinate high-spin Fe(III) to distorted square pyramidal Cu(II) in an assembly with Cu–F–Fe = 172°.[13,28] Curie–Weiss dependence is also observed (Figure 6); a linear least-squares fit of the data yields C = 4.88 emu K/mol and θ = 3.64 K. For the system of independent spins S = 5/2 and 1/2, C = 4.75 emu K/mol (g = 2). Consequently, negligible magnetic coupling is propagated across the [Fe^{III}–F–Cu^{II}] bridge. In an approximate sense, the copper magnetic orbital $\sigma^*(d_{x^2-y^2})$ is orthogonal to the superexchange-propagating orbitals of fluorine; this combined with the decidedly asymmetric dimensions (Fe–F = 1.865(3) Å, Cu–F = 2.101(3) Å) and long Cu···Fe separation (3.956(1) Å) leads to no significant interaction. With assembly [**3**]$^+$, the bridge is essentially linear, strong bridge bonds differ by only 0.07 Å, the Cu···Fe separation is 3.57 Å, and the antiparallel superexchange pathway Cu(d_{z^2})–O(s/pσ)–Fe(d_{z^2}) is evident. This bridge is well constituted to support the substantial antiferromagnetic coupling observed.

The EPR spectrum of [**3**]$^+$, silent in dichloromethane solution at 12 K except for trace high-spin Fe(III) and Cu(II) contaminants, is also consistent with the magnetic behavior. Further indication of the strong electronic coupling is evidenced by the paramagnetically shifted ^{1}H NMR signals of the OEP ligand, shown in Figure 8. These occur with significantly smaller isotropic shifts than typical high-spin Fe(III) porphyrins,[50,59] expected because the shifts are mainly contact in origin[50] and would scale with magnetic susceptibilities. Several shift comparisons with O-ligated high-spin hemes are provided in Table IV. The distinctive chemical shifts, along with the presence of diastereotopic methylene protons (split by 2.6 ppm), are persuasive evidence for retention of the bridge structure in solution.

Summary. The following are the principal results and conclusions of this investigation.

1. The oxo-bridged assembly [(OEP)Fe–O–Cu(Me$_6$tren)]$^+$ is readily prepared by the coupling of axially labile [Fe(OEP)(OClO$_3$)] and the terminal hydroxo species [Cu(Me$_6$tren)(OH)]$^+$ (generated in situ) in the presence of a suitable base. The reaction sequence of Scheme I in acetone solution affords [(OEP)Fe–O–Cu(Me$_6$tren)](ClO$_4$) in 70% yield together with a high-spin Fe(III) side product, presumably the enolate complex [Fe(OEP)(OCH(Me)=CH_2)], which is easily separated by differential solubility. This procedure eliminates the formation of [Fe(OEP)$_2$]O, a conceivable product sink in the coupling reaction. The trigonal bipyramidal structures of precursors [Cu(Me$_6$tren)(OH$_2$)]$^{2+}$ and [Cu(Me$_6$tren)(OH)]$^+$ have been proven by X-ray methods.

2. The existence of the [Fe^{III}–O–Cu^{II}] bridge unit, linking trigonal bipyramidal Cu(II) and tetragonal five-coordinate Fe(III), has been demonstrated by X-ray structural analysis of three different molecules in two crystalline forms. Deviations from the bridge mean parameters Fe–O–Cu = 176.7°, Fe–O = 1.745 Å, and Cu–O = 1.829 Å over the three structures are insignificant. Both structural and Mössbauer spectroscopic data establish the presence of high-spin Fe(III).

3. The synthesis of the assembly [(OEP)Fe–O–Cu(Me$_6$tren)]$^+$ allows the first comparison of electronic properties between the binuclear spin-coupled site in the "as-isolated" form of CcO and a structurally defined, electronically congruent synthetic analogue. Especially significant property convergences with the enzyme site are the antiferromagnetically coupled S = 2 ground state and the associated lack of an EPR signal at low temperatures.

(57) O'Connor, C. J. *Prog. Inorg. Chem.* **1982**, *29*, 203.
(58) For extensive plots of this type, *cf.*: Wojciechowski, W. *Inorg. Chim. Acta* **1967**, *1/2*, 324.
(59) Goff, H. M. In *Iron Porphyrins*; Lever, A. D. P., Gray, H. B., Eds.; Addison-Wesley: Reading, MA 1983; Part 1, Chapter 4.

4. Of the numerous prior synthetic approaches to the enzyme site, only those compounds with bridging thiolate (Fe^{III}–S(R)–Cu^{II}) in heme–bis(dithiolene) species are structurally well-defined.[25b-e] Putative oxo/hydroxo[21a,d] and chloride/bromide[21] bridged species do not enjoy (accurate) structural definition. These and the thiolate-bridged complexes do not necessarily contain $S = 5/2$ Fe(III) and exhibit weak or nil magnetic coupling compared to the enzyme site.

Given the results in 3, $[(OEP)Fe–O–Cu(Me_6tren)]^+$ may be described as a synthetic analogue of the binuclear site of oxidized CcO inasmuch as it reproduces the most idiosyncratic property of that site at present. In a future report, we will present a detailed spectroscopic characterization of the bridged assembly in comparison with electronic features of the enzyme site. At this point, we raise two caveats concerning the fitness of $[3]^+$ as an exact analogue. First, the Fe(III) site in $[3]^+$ is five-coordinate, whereas resonance Raman results point to a six-coordinate heme a_3 site.[11a] In this arrangement, the axial ligands are the bridge atom and, presumably, an imidazolyl group from histidine. Second, inasmuch as EXAFS results favor a monoatomic bridge,[5,17] possible candidates in addition to oxide include hydroxide, chloride, thiolate, and sulfide. There is no information concerning the magnetic or other properties of unsupported [Fe^{III}–X–Cu^{II}] bridges with these bridging atoms X. Future research will include an investigation of the stabilities of these bridge units.

Acknowledgment. This research was supported by NSF Grant CHE 9208387. X-ray difraction equipment was obtained by NIH Grant 1 S10 RR 02247. We thank Professor E. Münck for useful discussions.

Supplementary Material Available: X-ray structural information for the compounds in Table I: tables of crystal and intensity collection data, positional and thermal parameters, interatomic distances and angels (31 pages); tables of observed and calculated structure factors (100 pages). This material is contained in many libraries on microfiche, immediately follows this article in the microfilm version of the journal, and can be ordered from the ACS; see any current masthead page for ordering information.